Nuclear Engineering and Technology 50 (2018) 203–210

Contents lists available at ScienceDirect

Nuclear Engineering and Technology

journal homepage: www.elsevier.com/locate/net

Technical Note

Calibration of digital wide-range neutron power measurement channel for open-pool type research reactor☆

Sungmoon Joo [a, *], Jong Bok Lee [b], Sang Mun Seo [b]

[a] Decommissioning Technology Research Division, Korea Atomic Energy Research Institute, 111 Daedeok-daero 989Beon-gil, Daejeon 34075, Republic of Korea

[b] Research Reactor System Design Division, Korea Atomic Energy Research Institute, 111 Daedeok-daero 989Beon-gil, Daejeon 34075, Republic of Korea

ARTICLE INFO

Article history:
Received 7 June 2017
Received in revised form
29 September 2017
Accepted 28 October 2017
Available online 2 December 2017

Keywords:
Commissioning
Digital Wide-Range Neutron Power Measurement
Fission Chamber
Nuclear Instrumentation System
Power Calibration
Research Reactor

ABSTRACT

As the modernization of the nuclear instrumentation system progresses, research reactors have adopted digital wide-range neutron power measurement (DWRNPM) systems. These systems typically monitor the neutron flux across a range of over 10 decades. Because neutron detectors only measure the local neutron flux at their position, the local neutron flux must be converted to total reactor power through calibration, which involves mapping the local neutron flux level to a reference reactor power.

Conventionally, the neutron power range is divided into smaller subranges because the neutron detector signal characteristics and the reference reactor power estimation methods are different for each subrange. Therefore, many factors should be considered when preparing the calibration procedure for DWRNPM channels. The main purpose of this work is to serve as a reference for performing the calibration of DWRNPM systems in research reactors.

This work provides a comprehensive overview of the calibration of DWRNPM channels by describing the configuration of the DWRNPM system and by summarizing the theories of operation and the reference power estimation methods with their associated calibration procedure. The calibration procedure was actually performed during the commissioning of an open-pool type research reactor, and the results and experience are documented herein.

1. Introduction

The main purpose of research reactors is to produce neutrons. However, it is difficult to directly measure the number of neutrons produced during the reactor operation. The reactor thermal power can be used as an indicator of the amount of neutrons produced by the reactor because there is a proportional relationship between the neutron flux and the rate at which heat is produced in the reactor core.

There are some issues in using the reactor thermal power as a means to monitor the total reactor power. The thermal power responds slowly to power level changes because reactor inlet and outlet flow temperatures are used to calculate the thermal power. In addition, the thermal power may not be reliable in the very low-power region because the energy balance in this region can be easily perturbed by external disturbances.

Therefore, instead, the local neutron flux is measured and is mapped to the total reactor power through power calibration [1–3]. Power calibration is a process of mapping the neutron flux signal to the reference power signal. During reactor operation, frequent calibration is required to accommodate occasional changes of the core arrangement and the associated flux distribution [2]. Power calibration is also a critical part of reactor commissioning because the nuclear instrumentation system should be accurately calibrated in order to check whether the reactor's performance and safety requirements are met [4].

Fig. 1 shows a typical neutron flux measurement range for the out-of-core (or ex-core) neutron detectors [5]. The measurement range is over 10 decades and is typically divided into three subranges: source (or start-up) range, intermediate range, and power range. Reliable reference powers for calibration are different for each power range, and therefore, a different power calibration method is required for each power range [2,3].

Traditionally, several power calibration methods have been adopted. Each method has its own limitations, advantages, and appropriate power range of application [2,3]. Unlike nuclear power plants, which have dedicated neutron detectors for each power range, it is common for research reactors to use a single wide-range detector that covers the entire range of power measurement.

☆ All authors have contributed to the paper and have never submitted the manuscripts, in whole or in part, to other journals.

* *Corresponding author.*
E-mail address: smjoo@kaeri.re.kr (S. Joo).

https://doi.org/10.1016/j.net.2017.10.011

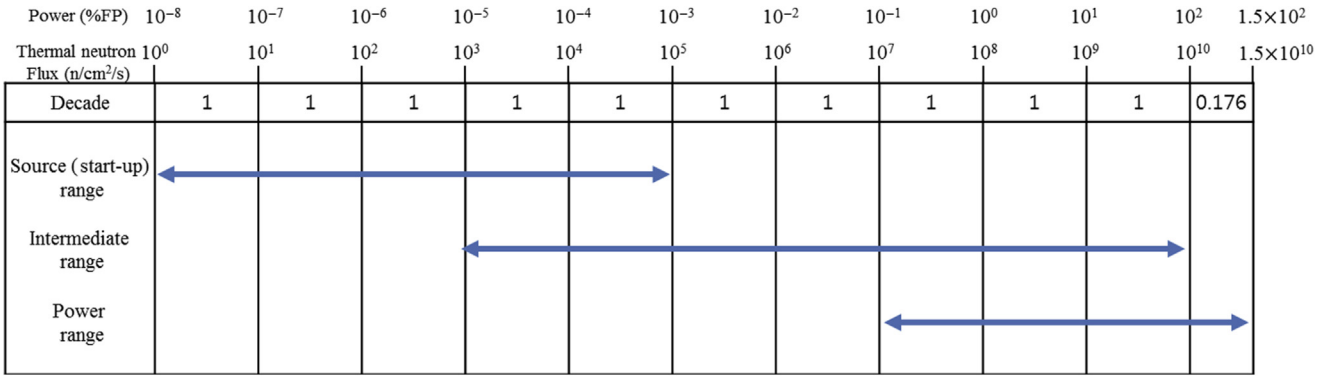

Fig. 1. Typical ranges covered by out-of-core wide-range neutron detectors.

This makes the power calibration for research reactors more complicated.

Another aspect of calibration to consider is the type of instrumentation, analog or digital. Even though the adaptation of digital nuclear instrumentation is not a requirement, the modernization of nuclear instrumentation is an unavoidable trend [6]. Digital nuclear instrumentation systems, in general, have improved performance in terms of accuracy, signal-processing capability, and reliability. Compared with conventional analog instrumentation systems, digital instrumentation systems are easy to calibrate and have reduced calibration and maintenance requirements [6].

There has not been much work on describing the overall calibration procedure for digital wide-range neutron-power measurement (DWRNPM) channel in research reactors because most of the previous studies on power calibration have focused on a specific power range. The motivation for this article was to fill this information gap by making the following contributions: (i) providing readers with a comprehensive overview of calibration over the entire measurement range by describing the configuration of typical DWRNPM channels, (ii) summarizing the theories of operation and the neutron power calibration methods for each subrange, and (iii) sharing actual experience from calibration during commissioning of an open-pool type research reactor.

The remainder of this article is organized as follows: Section 2 describes the configuration and the theories of operation of DWRNPM channels. In Section 3, calibration methods for low- and high-power regions are summarized. The implementation of calibration procedures and results of actual power calibration during the commissioning of a research reactor are documented in Section 4. Finally, we conclude the article in Section 5.

2. Description of the digital wide-range neutron power measurement channel

Fig. 2 illustrates a schematic diagram of a typical DWRNPM channel [1,7]. This section identifies the major functional components in the channel and describes their operation.

2.1. Neutron detector: wide-range fission chamber

The nuclear fission rate is proportional to the thermal neutron flux density. In the low-power region, neutron flux density is so low that the fissioning is detected in the form of discrete electrical pulses. On the other hand, in the high-power region, the rate of fissioning is so high that the neutron flux can be detected in the form of an electrical current that has direct current (DC) component and/or alternating (fluctuating) current (AC) component.

To handle this wide measurement range with a single detector, fission chambers are commonly used because fission chambers are operable in both pulse-generating mode and current-generating mode [1,5].

Fig. 3 illustrates the concept of the fission chamber operation. The facing surfaces of the high voltage and signal electrodes have a uranium conversion layer. The main composition of the conversion layer is U-235; however, small amounts of unwanted isotopes such as U-234 are also present [5,7]. The space charge region between the coated electrodes is occupied with a high-purity gas blend (e.g., argon and nitrogen) [5,7].

When the entering neutrons interact with and fission the U-235 coating, energized fragments are injected into the space charge region. These energetic fragments ionize the atoms in the gas volume and electrons are liberated, forming positive ions. However, the detector signal generated at low reactor power may not be a direct measure of only a neutron-induced reaction because a fission chamber is also sensitive to other ionizing radiations, such as gamma ray and alpha particles [5].

2.2. Signal processing and calibration

The signal from the detector is in the form of electrical pulses or (DC and AC) current. The signal is further processed by a series of electronic circuits and/or software algorithms to convert the neutron flux signal to a reactor power signal. This section describes the characteristics of the neutron flux signal, the algorithms required to process the signal, and how the signal is converted to a neutron power signal.

2.2.1. Signal modes and the Campbelling technique

In general, neutron detectors may be designed for any of the two distinct modes of operation: pulse-generating mode and current-generating mode. One of the features that make fission chambers suitable for wide-range power measurement is that they are operable in both modes. Whereas it is relatively simple to process the signal from a detector in pulse-generating mode, a special technique is required for the signal in current-generating mode.

The amplitude of the electrical pulse resulting from a neutron-induced fission process is larger than that of a pulse resulting from the other competing nuclear reactions (e.g., gamma ray, alpha particle). A pulse height discrimination process uses this characteristic and selectively passes the neutron-induced pulses by rejecting the pulses below a preset threshold. Beyond the pulse-generating range, the detectors operate in the current-generating mode. The signal in the current-generating mode can be processed efficiently by applying Campbell's theorem [5].

In most cases, pulse-generating mode operation is limited to rates below approximately 10^5 counts per second (cps) [5]. As the pulse rate increases, individual pulses cannot be detected because of the overlapping of the pulses. The result is a fluctuating current,

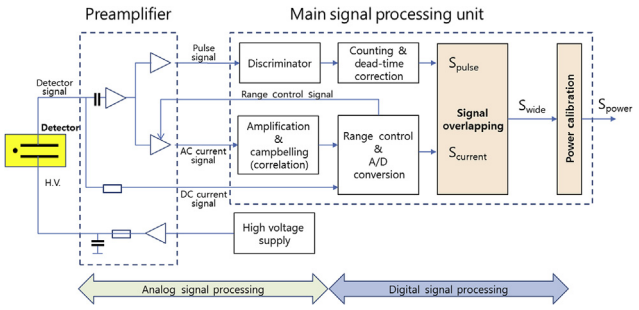

Fig. 2. Schematic of the digital wide-range neutron power measurement channel.

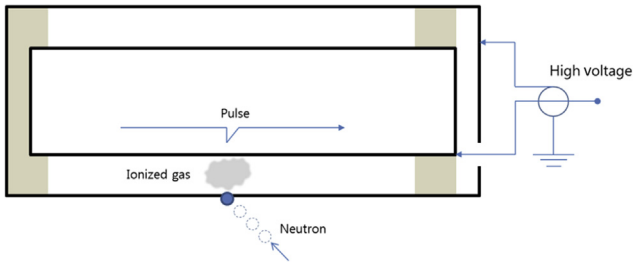

Fig. 3. Fission chamber operation concept.

and the neutron detectors enter current-generating mode. The leakage currents in the detector insulation and cable dielectric material determine the starting points or the lower limits of current mode operation [5]. Unlike pulse mode operation, all pulses in current mode, regardless of pulse height, contribute to the resulting current signal, and the benefit of pulse height discrimination is lost. One method of compensating this loss is the use of Campbell's theorem.

Campbell's theorem states that the variance of the detector current, I(t), is proportional to the average pulse rate and the mean square charge per pulse, as shown in Eq. (1)

$$\overline{\sigma_I^2(t)} \overset{\text{def}}{=} \frac{1}{T}\int_{t-T}^{t} [I(\tau) - I_0]^2 d\tau = \frac{\overline{n}Q^2}{T} \tag{1}$$

where $\overline{n}$ is the average pulse rate and Q is the mean charge per pulse.

It is worth noting that, by applying Campbell's theorem, radiations with smaller pulses and noises are filtered out because the larger pulses produce a greater contribution to the mean square value of the current due to the squared terms. This mode of operation is known as the mean square voltage mode or Campbelling mode.

Above the mean square voltage mode, the signal depends mainly on the DC signal output. Campbell's theorem states that the mean value of the current, $\overline{I(t)}$, is a good measure of the neutron flux. The mean value of the neutron-induced current is given by Eq. (2) for the DC region.

$$\overline{I(t)} = I_0 = \overline{n}Q \tag{2}$$

Theoretically, the current signal in the DC region is the aggregated sum of the responses to neutron and other competing radiations. However, the neutron response is significantly predominant, and the contributions from other radiations—mainly gamma ray—are considered negligible in practice [5,7].

2.2.2. Normalization, overlapping, and power calibration

In the main signal-processing unit in Fig. 2, the pulse and current signals coming from the wide-range preamplifier are conditioned, digitized, and numerically merged into the wide-range signal. The pulse signal is shaped by a discriminator with an adjustable threshold and is transmitted to a counter. The AC current signal is amplified by a wide-band amplifier with selectable measurement ranges and is processed. In the current correlator, the signal is processed in accordance with Campbell's theorem. The output signal is digitized and transmitted to the microprocessor for further digital signal processing. The current signal and the pulse signal are merged by an overlapping algorithm, yielding a wide-range signal. The wide-range signal is then multiplied by a power calibration factor.

Typically, there are four key parameters for the calibration of the DWRNPM channel: the current normalization parameter, the start point of the overlapping region, end point of the overlapping region, and the power calibration factor [7,8].

The current normalization parameter, C_{norm}, is a multiplicative parameter used to convert the detector current signal to the normalized current signal,

$$S_{current} = C_{norm} \cdot D_{current} \tag{3}$$

where $S_{current}$ is the normalized current signal, and $D_{current}$ denotes the detector current signal.

The value of the normalization parameter is chosen such that the normalized current signal and pulse count signal are properly aligned in the overlapping region, as shown in Fig. 4 [8].

The overlapping region of the pulse signal (S_{pulse}) and current signal ($S_{current}$) is used for signal selection and interpolation. The overlapping region can be characterized by two adjustable parameters, the start point of the overlapping region ($S_{start,}$) and the end point of the overlapping region (S_{end}). The following is an example of the overlapping algorithm to determine the wide-range signal (S_{wide}),

$$\begin{aligned} S_{wide} &= S_{pulse} \text{ for } S_{pulse} < S_{start} \\ S_{wide} &= \alpha * S_{pulse} + (1-\alpha)\, S_{current} \text{ for } S_{start} < S_{pulse} < S_{end} \\ S_{wide} &= S_{current} \text{ for } S_{pulse} > S_{end} \end{aligned} \tag{4}$$

where $\alpha = (S_{end} - S_{pulse})/(S_{end} - S_{start})$

As mentioned in Section 2.2.1, the pulse mode operation is limited to rates below approximately 10^5 cps, which can provide a guidance to determine the value of S_{start}. The parameters $S_{start,}$ and S_{end} are

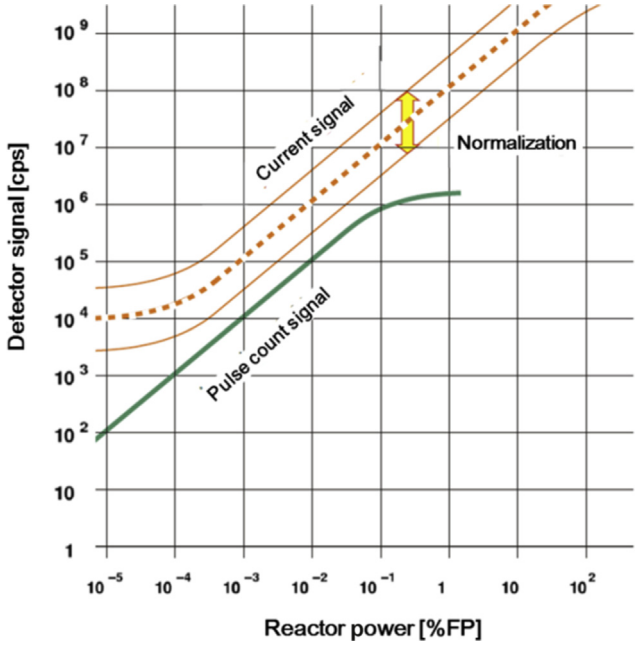

Fig. 4. Detector current normalization.

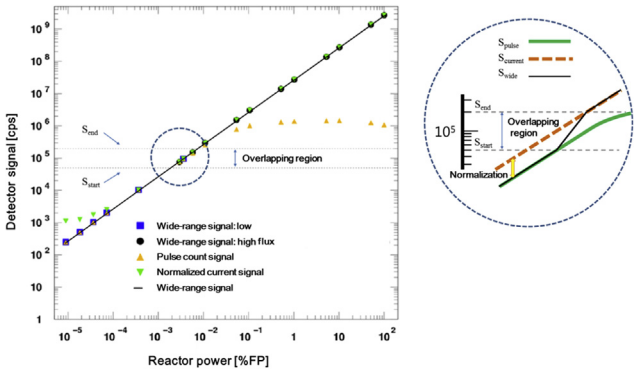

Fig. 5. Detector signal overlapping.

determined such that the wide-range signal is continuous and monotonically increasing with the reactor power as shown in Fig. 5 [8].

The power calibration factor is defined by Eq. (5).

$$c_{\mathrm{cps\_to\_\%FP}} = \frac{100\%FP}{S\,(100\%FP)}\,[\%FP/\mathrm{cps}] \tag{5}$$

where S (100% FP) denotes the measured wide-range signal (unit cps) at 100% FP power level.

Finally, the power signal is obtained by Eq. (6).

$$S_{power} = c_{\mathrm{cps\_to\_\%FP}} \cdot S_{wide} \tag{6}$$

Neutron power calibration is the process of adjusting the power calibration factor ($c_{\mathrm{cps\_to\_\%FP}}$). This is done by multiplying the appropriate scaling factor to the power signal; given an initial calibration factor for a channel, a new calibration factor is determined by the following procedure:

Step 1: Power up the reactor to a known reference power level (e.g., 100% FP).

Step 2: Record the displayed reactor power.

Step 3: New calibration factor = initial calibration factor × reference reactor power/displayed reactor power.

The calibration of the digital neutron power measurement channels can be easily performed by updating the numerical values of the calibration factors, whereas the calibration of the analog nuclear instrumentation systems often involves adjusting the circuit elements [3].

2.2.3. Signal scaling and signal-sourcing strategy

In practice, a current of 4–20 mA is used to transmit the wide-range power signal, which is over 10 decades. Therefore, proper scaling of the signal is critical to preserve measurement accuracy. The following is an example of the linear scale and logarithmic scale current signal representation of the power range between 10^{-8}% FP and 150 % FP,

$$\text{Linear scale power signal: } 4 + 16 \times \frac{\mathrm{Power}[\%FP] - 10^{-8}}{150 - 10^{-8}}\,[\mathrm{mA}] \tag{7}$$

$$\text{Logarithmic scale power signal: } 4 + 16 \times \frac{Log(\mathrm{Power}[\%FP]) - Log(10^{-8})}{Log(150) - Log(10^{-8})}\,[\mathrm{mA}] \tag{8}$$

A power change from 10% FP to 150% FP in Eq. (7) yields a change of approximately 15 mA, as shown in Fig. 6. This change of 15 mA will provide sufficient sensitivity for controlling the reactor power or triggering the reactor protection system (RPS) in the power range between 10% FP and 150% FP. On the other hand, the linear scale signal changes only approximately 1 mA, whereas the power

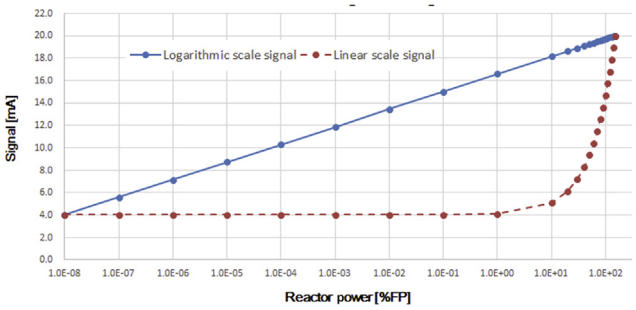

Fig. 6. Comparison of signal scaling.

level has changed 9 decades from 10^{-8}% FP to 10% FP. Therefore, the sensitivity of the linear scale signal is very low in this range.

Instead, a change in power from 10^{-8}% FP to 10% FP yields a change of approximately 14 mA if the logarithmic scale in Eq. (8) is used. One caveat with using the logarithmic scale is that the response will flatten, and it loses the signal sensitivity as the power level rises above 10% FP, as shown in Fig. 6. This implies that the two scales are complementary to each other.

A common signal-sourcing strategy to accommodate the complementary characteristic of the signal sensitivity is to use the linear scale power over the last decade of power level to allow close monitoring of the reactor in the intermediate or high-power range, and the logarithmic scale power can be used for the lower decades.

3. Neutron power calibration methods

This section summarizes the three reference power estimation methods and their associated calibration procedures, two for the low-power region and one for the high-power region.

3.1. Power calibration in the low-power region

At microwatt or milliwatt power levels, the kinetic parameter and power conversion factors to convert the count rates of the reference neutron detectors [e.g., boron trifluoride (BF_3) proportional counters] to the fission power can be derived from the variance to mean ratio (VTMR) analysis of the neutron pulse signals at a subcritical stationary condition [9,10]. By using calibrated reference neutron detectors, the average fission rates (fission/sec) are measured, and the fission power levels are determined by multiplying the conversion factor (e.g., 200 MeV/fission) with the fission rates. Once the fission power is determined, the signal from the neutron power measurement channels can be calibrated accordingly.

At kilowatt power levels, the fission power can be determined by comparing the measured reaction rate of the gold (Au) test specimens with the calculated reaction rate at a certain power level. The neutron absorption rate distribution is measured through the activation analysis of the irradiated Au test specimens. The measured neutron absorption rate distribution is compared with the calculated results.

The reactor power is raised to a certain level to activate the test specimens to the appropriate radioactivity level for the measurement. After a sufficiently long duration of reactor operation at a certain power level, the reactor is shutdown, and the specimens are withdrawn. The relative radioactivity distribution at a reference timing is measured for each specimen by gamma scanning. The specimen is cut into small pieces after the gamma scanning is complete, and the absolute radioactivity of each piece is measured. Then, the neutron absorption reaction rate during irradiation is calculated from the absolute radioactivity [10].

Based on the relative radioactivity distributions and the neutron absorption rate distribution of the specimen, the neutron

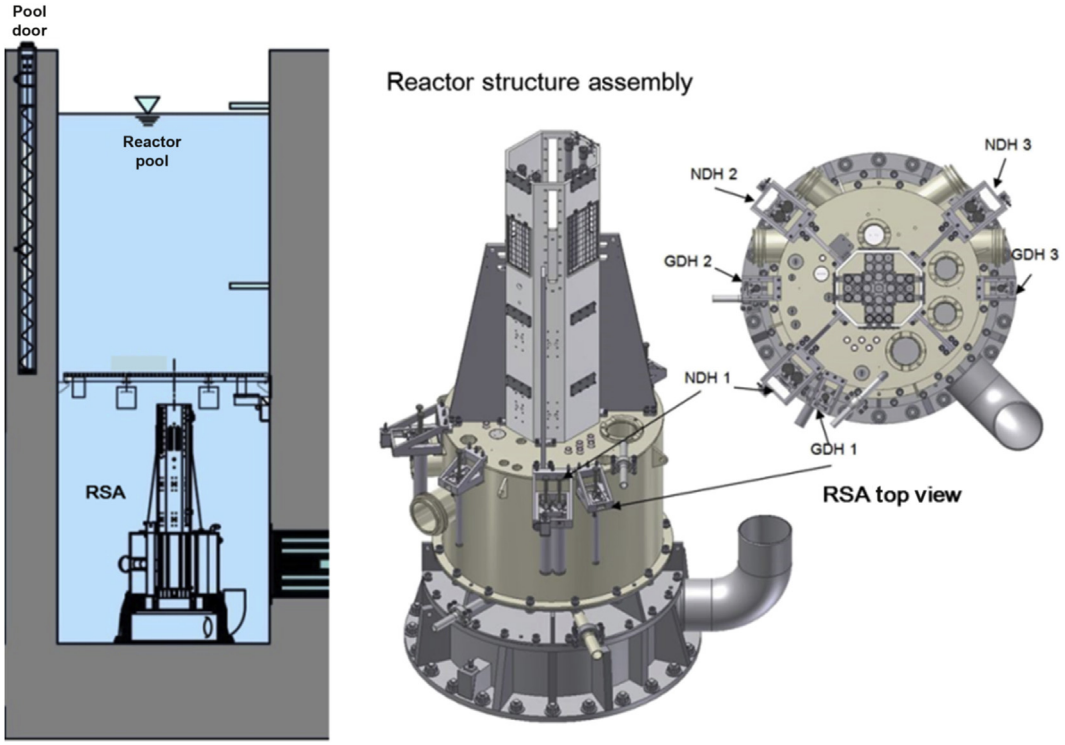

Fig. 7. Reactor structure assembly and detector housing.

absorption rate distributions of the specimen are determined. The neutron absorption rate distributions are compared with the calculations, and the fission power during the irradiation is estimated. The neutron power measurement channels can be calibrated using the estimated fission power as a reference power.

3.2. Power calibration in the high-power region

In the high-power region, the calculation of thermal power using a thermal heat balance is considered reliable and can be used as a reference power for calibration. This section describes the calibration procedure using the calculated thermal power in the high-power region.

As a prerequisite, preliminary calibrations must be performed on the logarithmic and linear scale neutron power signals at the low-power region using the methods described in Section 3.1.

The energy generated in the core consists of fission energy and decay heat. The decay heat is considered negligible during the test with fresh fuels or when starting the reactor operation after a long period of shutdown because it takes some time for the decay heat to buildup. Therefore, for all practical purposes, the energy generated in the core is considered to be proportional to the neutron population in the core. Most energy is transferred to the primary coolant and some to auxiliary systems connected to the reactor.

The reactor thermal power in a stationary state can be calculated by summing all the thermal powers removed by the systems connected to the reactor, as shown in Eq. (9).

$$Q_{th} = \sum_{i=1}^{m} Q_{th,\ i} = \sum_{i=1}^{m} \dot{m}_i C_{p,i} \Delta T_i \tag{9}$$

where $Q_{th,}$[W] is the total thermal power generated in the reactor, $Q_{th,i}$[W] is the thermal power removed by the ith system connected to the reactor, $\dot{m}_i$[kg/s] is the mass flow rate of the ith system, $C_{p,i}$[J/kg K] is the constant pressure specific heat of the ith system, and ΔT_i[K] is the difference between the inlet flow temperature and outlet flow temperature of the ith system.

The thermal power calculation may begin from 10% FP or 20% FP, and the reactor power is increased stepwise by 10% FP or 20% FP. At each step of power increase, the power level at the next step is predicted. If any channel of the power signals is predicted to exceed 100% FP at the next step, the power channel is calibrated to the thermal power of the current step. Otherwise, the stepwise power increase continues to 100% FP without additional calibration, ignoring small allowable calibration errors in the power signal channels.

When the power demand (PDM) to the reactor regulating system (RRS) is 100% FP and the reactor is in a stationary state, the thermal power is calculated, and the deviation between the displayed neutron power of each channel and the calculated thermal power must be checked. If the deviation is larger than the acceptance criteria, the power calibration factor is required to be updated as described in Section 2.2.2.

After calibrating the neutron power channels at a PDM of 100% FP, the calibration is reconfirmed at several power levels (e.g., 80%, 60%, 40%, and 20% FP), while the power is decreased stepwise. The power decrease continues to the source range. In the low-power region, however, interchannel deviation is more important than the actual deviation between a neutron power channel reading and the calculated thermal power because the calculated thermal power may not be reliable.

4. Implementation of the neutron power calibration

The power calibration methods described in Section 3 were applied to an open-pool type multipurpose research reactor recently built and commissioned by the Korea Atomic Energy Research Institute. The reactor reached its first criticality in April 2016 and reached full power in September 2016 during the commissioning. This section describes the procedure and the results of the neutron power calibration performed during the commissioning.

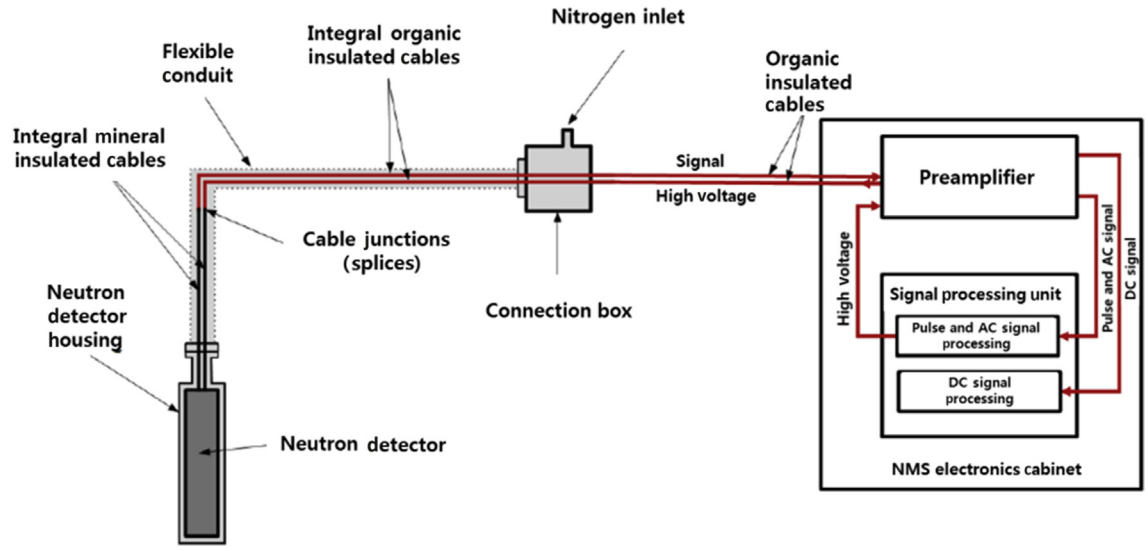

Fig. 8. Neutron power measurement channel.

4.1. Overview of the reactor and neutron measurement system

The nominal thermal power of the reactor is 5 MW. The reactor uses box-type fuel assemblies with flat fuel plates. The fuel for the equilibrium core is low-enriched uranium. Light water functions as both the coolant and moderator inside the reactor pool. Fig. 7 illustrates the reactor structure assembly (RSA) and the detector housings in which detectors are installed.

There are three channels of neutron detectors for the RPS and three channels of neutron detectors for the RRS installed around the RSA. These six neutron detectors comprise the neutron measurement system (NMS) of the reactor. Wide-range fission chambers are used to measure the thermal neutron flux. Each channel of the NMS is composed of a detector, a preamplifier (signal-conditioning unit), and a signal-processing unit, as shown in Fig. 8. Neutron detectors are installed inside neutron detector housings (NDHs) 1, 2, and 3. The detectors for RRS Channel A and RPS Channel A are installed inside NDH 1. Similarly, the detectors for Channel B and C are installed inside NDH 2 and NDH 3, respectively. The position of the NDH is adjustable, and the nominal position of each NDH is determined such that the neutron flux level at 100% FP is 10^{10} nv.

In addition, around the RSA, three channels of gamma detectors are installed, making up the reactor gamma monitoring system (RGMS). The RGMS uses gamma ionization chambers to detect unsafe transitions or fuel failures. The gamma detectors are installed inside gamma detector housings 1, 2, and 3. Other radiation detectors, which are neither installed around the RSA nor a part of the NMS, are beyond the scope of this article.

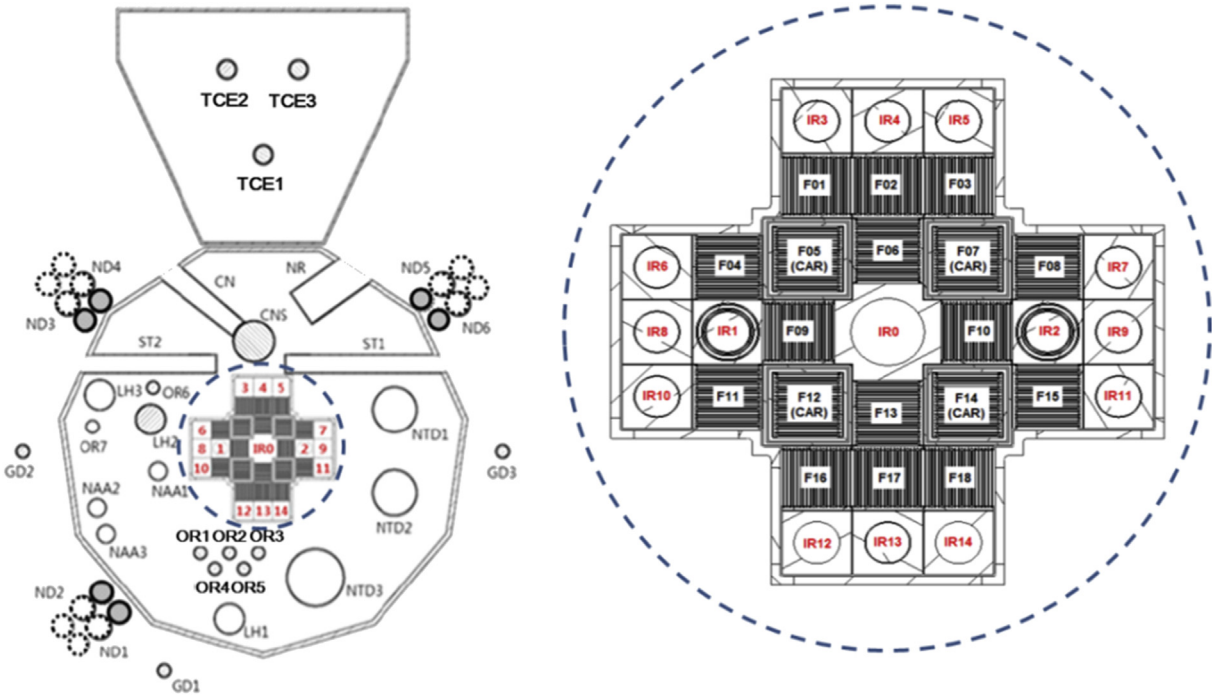

Fig. 9. Fuel loading and irradiation test holes.

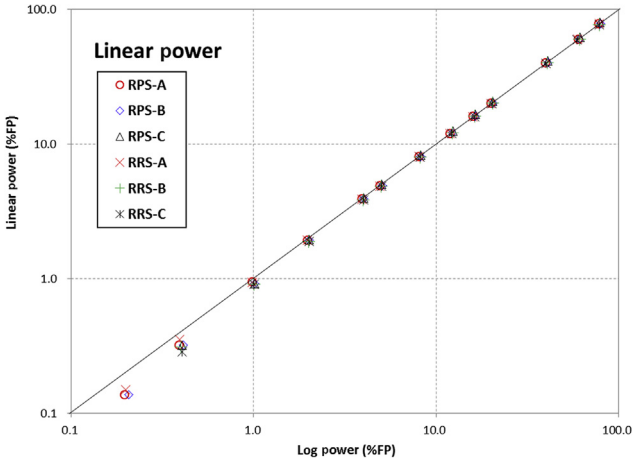

Fig. 10. NMS linear power versus logarithmic power before calibration.

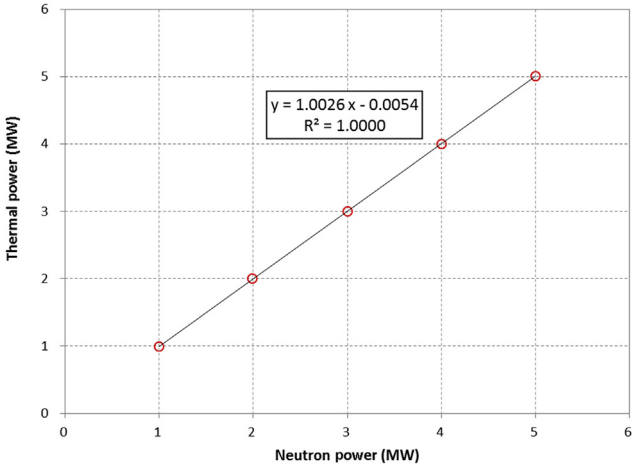

Fig. 11. Thermal power versus neutron power after calibration.

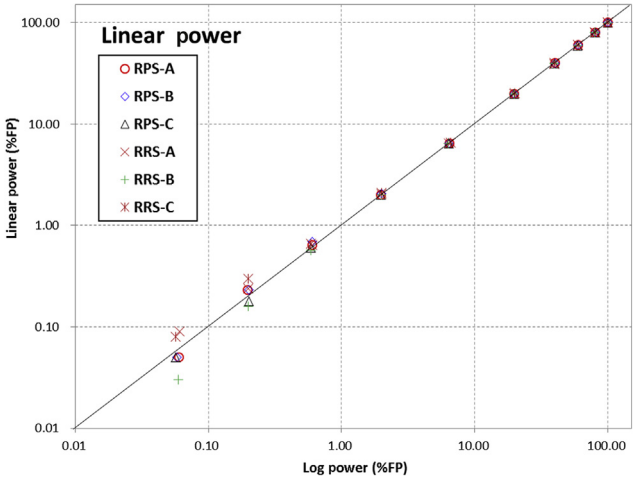

Fig. 12. NMS linear power versus logarithmic power after calibration.

4.2. Overall calibration procedure

Neutron power calibration is performed after the preliminary calibrations using the VTMR method and the Au specimen irradiation method described in Section 3.1.

During the neutron power calibration, all neutron channels are measured while the reactor is in a stationary state at each level of PDM. The thermal power measurement begin at a PDM of 1 MW (20% FP), and the PDM is increased up to 5 MW, in steps of 1 MW. If the predicted neutron power signal at the next step is sufficiently lower than 5 MW until a PDM of 3 MW, the PDM is increased without additional calibrations.

At a PDM of 4 MW, which is the last PDM before reaching 100% FP, all channels require a check to determine if the deviation between the reference thermal power and the NMS power reading is larger than the acceptance criteria. Preliminary calibrations can be performed at a PDM of 4 MW, if necessary. The final calibration is performed at a PDM of 5 MW. The calibration of the neutron power channels is reconfirmed while the PDM is decreased stepwise.

4.3. Results and discussion

4.3.1. Preliminary calibration in the low-power region

While measuring the kinetic parameter (β/Λ) and the flux distribution during the commissioning, the reactor powers were estimated, and the neutron detectors were preliminarily calibrated.

Initially, two BF_3 counters were installed at OR3 and OR5 (see Fig. 9), and neutron signals were collected while adjusting the control rod positions near the criticality condition. The data analysis yielded the kinetic parameter and the power conversion factors of the two BF_3 counters at OR3 and OR5. This process was repeated while moving the detectors to TCE2 and TCE3 holes and then the NMS channels were checked. The power conversion factors at the OR and TCE holes were approximately 2.0E-8 W/cps and 5.0E-6 W/cps, respectively. The estimated reactor powers were at microwatt levels, and the preliminary neutron power calibration of the NMS channels was performed accordingly.

The flux distribution measurement test is to measure the thermal neutron flux distribution of the reactor core in the low-power region to check the deviation in the flux distribution between prediction and measurement. While the neutron flux distribution was measured through the activation of Au wires and foils, the fission power during the irradiation was estimated. Au wires and foils were installed at five FAs and two RI capsules in the IR0 (Fig. 9) and then irradiated at a PDM of 2 kW for approximately 8 hours. The wires and foils were withdrawn after reactor shutdown, and the relative radioactivity distribution was measured by gamma scanning.

The absolute neutron flux was determined by the activities of the Au specimens at each irradiation position. The true fission power was determined by comparison of the measured reaction rate with the calculated reaction rate. The true reactor power during the irradiation was estimated to be 1.801 kW, and all the NMS channels were calibrated to this power before the neutron power calibration in the high-power region.

4.3.2. Neutron power calibration in the high-power region

Fig. 10 illustrates the neutron power measurements before calibration during the stepwise power ascension. The negative offsets for the power levels below 1% FP were observed. These negative offsets are believed to be mainly due to nonlinearities in the electronics and numerical signal processing, which were also observed in HANARO [3].

The calibration at a PDM of 4 MW was omitted because the deviations between the NMS channel measurements and the calculated thermal reference powers were within the acceptance criteria. When all six NMS channels were calibrated at a PDM of 5 MW, following the procedure in Section 2.2.2, it was found that the calculated thermal power was 6.8% higher than the average of the NMS channel readings.

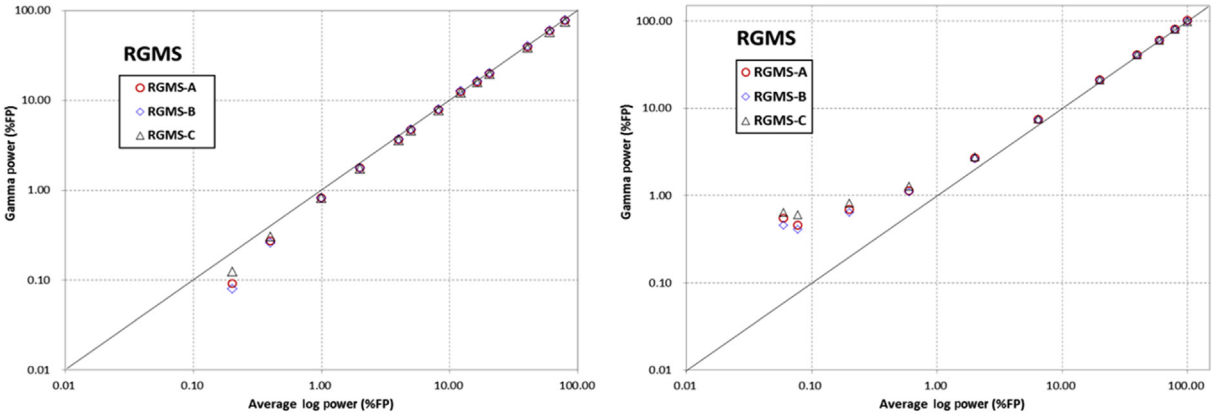

Fig. 13. Effect of the delayed gamma radiation.

The neutron power calibration was verified by measuring the neutron powers during the stepwise power descent. Fig. 11 illustrates the result, which shows that the calibration was successful.

Our signal-sourcing strategy for the RRS was as follows: when the power is increasing, the neutron power is represented by the NMS logarithmic power until it increases up to 6.9% FP, and when the power is decreasing, the transition from the linear scale power to logarithmic scale power occurs at 6.4% FP (refer to Section 2.2.3 for details). To verify the smooth transitions between the logarithmic and linear scale signals, differences between the two power scales were assessed near the transition points. The differences were well within the acceptance criteria, falling between 0.04% FP and 0.18% FP for all six NMS channels.

Fig. 12 illustrates the NMS linear scale power versus NMS logarithmic scale power during the power descent after the neutron power calibration at 5 MW. The negative offsets shown in Fig. 10 were almost compensated. Actually, positive offsets were observed in some channels, and they were believed to be mainly due to the effect of the delayed gamma radiation; a linear power signal consists of neutron power and gamma power, and the gamma power is composed of prompt gamma power and delayed gamma power. Among these power compositions, the effect of the delayed gamma radiation becomes noticeable in the low-power region after a certain period of reactor operation.

To verify the hypothesis, the gamma power channels in the RGMS were checked. The RGMS power signal consists of prompt gamma power and delayed gamma power. Therefore, the effect of the delayed gamma radiation was expected to be more apparent in the RGMS than in the NMS. The RGMS signals for two cases were collected: Case 1 is the RGMS signal from stepwise power ascension right after the reactor start-up, and Case 2 is the RGMS signal from stepwise power decent after a certain period of reactor operation. Fig. 13 shows the comparison, which supports the hypothesis.

5. Conclusions

The main purpose of this work was to present a technical note that could serve as a reference for those who perform calibrations for research reactors, by providing a comprehensive overview of the calibration of a DWRNPM channel and by sharing actual experience from a calibration during the commissioning of a research reactor.

To provide background information, the configuration and operational theories of the neutron power measurement channel were described. In addition, the neutron power calibration procedures for the low- and high-power regions were summarized. The calibration procedures were performed during the commissioning of an open-pool type research reactor designed and built by the Korea Atomic Energy Research Institute.

The first calibration was performed at the microwatt level using the power estimated by the VTMR method. Then, the reactor power was raised to a PDM of 2 kW, and the actual power level was estimated to be 9.95% lower than the PDM. After the second calibration at a PDM of 2 kW, the final calibration was performed at a PDM of 5 MW, which showed that the calculated thermal power at a PDM of 5 MW was 6.8% higher than the average readings of the NMS channels. The final calibration was verified during a stepwise power descent.

Conflicts of interest

The authors have no conflicts of interest to declare.

Acknowledgment

This work was supported by the Research Reactor Instrumentation and Control Design grant funded by the Korea Atomic Energy Research Institute.

Appendix A. Supplementary data

Supplementary data related to this article can be found at https://doi.org/10.1016/j.net.2017.10.011.

References

[1] IAEA-TECDOC-973, Research Reactor Instrumentation and Control Technology, 1995.
[2] Eiji Suzuki, A Method for measuring absolute reactor power through neutron fluctuation, J. Nucl. Sci. Technol. 3 (3) (1966) 98–105.
[3] T. Kang, Y. Kin, B. Lee, S. Park, A study on the linearity characteristics of neutron power measurement system for HANARO, KAERI/TR-1338/99, 1999.
[4] Commissioning for Nuclear Power Plants, IAEA Safety Standard Series No. SSG-28, 2014.
[5] G.F. Knoll, Radiation Detection and Measurement, fourth ed., John Wiley & Sons, Hoboken, NJ, USA, 2010.
[6] Digital Instrumentation and Control Systems in Nuclear Power Plants: Safety and Reliability Issues, National Academy Press, Washington, D.C, 1997.
[7] Mirion Technologies, Technical data sheets for NMS, Doc. No. 023430-2-4-10, 2013.
[8] Mirion Technologies, Qualification reports for NMS, Doc. No. 023430-5-3-10-1, 2015.
[9] R.P. Feynman, F. De Hoffmann, R. Serber, Dispersion of the neutron emission in U-235 fission, J. Nucl. Energy 3 (1956) 64–69.
[10] H. Kim, H.R. Kim, K.H. Lee, J. Lee, Design characteristics and startup tests of HANARO, J. Nucl. Sci. Technol. 33 (7) (1996) 527–538.